Spin-resolved photoemission and *ab initio* theory of graphene/SiC

D. Marchenko,* A. Varykhalov, M. R. Scholz, J. Sánchez-Barriga, and O. Rader
Helmholtz-Zentrum Berlin für Materialien und Energie, Elektronenspeicherring BESSY II, Albert-Einstein-Straße 15, 12489 Berlin, Germany

A. Rybkina and A. M. Shikin
Institute of Physics, St. Petersburg State University, 198504 St. Petersburg, Russia

Th. Seyller
Technische Universität Chemnitz, Institut für Physik - Technische Physik, Reichenhainer Straße 70, 09126 Chemnitz, Germany

G. Bihlmayer
Peter Grünberg Institut and Institute for Advanced Simulation, Forschungszentrum Jülich and JARA, 52425 Jülich, Germany
(Received 13 October 2010; revised manuscript received 5 April 2013; published 16 August 2013)

The spin-orbit splitting of graphene π states can be strongly enhanced by external influences such as corrugation or proximity to heavier atoms. Here we investigate experimentally and theoretically whether such strong enhancement is possible for graphene on SiC(0001). By spin- and angle-resolved photoemission we found for two independently grown samples no resolvable spin-orbit splitting with an upper limit of our analysis of 20 meV. Our *ab initio* calculations predict a low spin-orbit splitting of 0.05 meV with small anisotropy but a local tenfold enhancement where hybridization with SiC substrate bands occurs.

DOI: 10.1103/PhysRevB.88.075422 PACS number(s): 81.05.ue, 71.70.Ej, 79.60.Dp, 73.20.At

Graphene displays fascinating electronic properties[1] with carrier mobilities of over 100 000 $cm^2/(V\,s)$ near room temperature[2] due to its π electrons. In momentum space they form a quasirelativistic energy dispersion around the Fermi energy termed the Dirac cone. The π electrons are also responsible for the potential use of graphene in spintronics.[3] First of all, there is the possibility of ferromagnetic ordering which has been reported for various graphitic carbon samples.[4–7] X-ray magnetic circular dichroism at the carbon K edge has been used to determine the aligned orbital magnetic moment.[7–9] Values of $5 \times 10^{-4} - 1 \times 10^{-3}$ μ_B per carbon atom have been obtained.[7] Ferromagnetic coupling can also be induced by proximity to 3*d* ferromagnets as occurs in multilayers: In 5.5-Å-C/25.5-Å-Fe heterostructures, an orbital magnetic moment of $0.05\mu_B$ per carbon atom has been determined at room temperature.[8] The same order of magnitude, 0.05–0.1 μ_B, has recently been found for catalytically grown graphene/Ni(111).[9] In this system, the Dirac cone of the graphene is found to be intact despite strong hybridization with the Ni substrate.[10]

Secondly, there is agreement that the spin-orbit interaction in graphene and graphite is very low in the valence band, even though the different calculations provide very different numbers.[11–13] Recent investigations obtained 0.05 meV (Ref. 12) and 0.024 meV.[13] The intrinsic spin-orbit coupling can contribute to a band gap at the Dirac point in various ways[14] with the contribution from carbon *d* states[15] being the dominating one.[13] Long spin relaxation lengths of 1–2 μm have been measured in free-standing graphene,[16] and by spin injection from a ferromagnet, spin valves have been realized from this material.[16–18]

Thirdly, the spin-orbit splitting can be enhanced by modification of graphene. This is achieved by introducing a curvature[19,20] with an extreme example being the carbon nanotube where a spin-orbit splitting of 0.37 meV has been measured.[20] Alternatively, a strong source of enhancement is proximity to a heavy element. In the system graphene/Au/Ni(111) a spin-orbit splitting of ∼13 meV has been measured by spin- and angle-resolved photoemission.[21] At the same time, the intercalated Au monolayer preserves the Dirac cone of ideal graphene.[21] The enhanced spin-orbit interaction in graphene with its steep and linearly dispersing π band is very interesting for spintronics because of the Rashba effect. This manifestation of the spin-orbit coupling leads to a splitting of the $E(k)$ valence band dispersion in momentum and energy. As a consequence, in two-dimensionally confined electronic systems, the Rashba-type spin-orbit coupling enables spin currents to be generated by electric fields,[22,23] thus allowing for the dissipationless transport of spin information.

For graphene, the effect of an external Rashba coupling on the Dirac cone at the $\overline{K}$ point of the Brillouin zone has been calculated analytically[24,25] as well as by density functional theory.[13,26] The modification to the band structure is that of a splitting into two concentric Dirac cones, a gapped and a nongapped one (see Fig. 3 in Ref. 25).[24,25] Consideration of higher-order terms modifies the Rashba effect on graphene.[14,27,28] The fine structure around the Dirac point is, however, not accessible by photoemission since the Au introduces a slight *p* doping in the graphene, moving the Dirac point just above the Fermi level.[29]

Recently, a giant spin splitting has been measured for graphene/SiC(0001).[30] This system, in which graphene becomes *n* doped, was the first from which the Dirac cone could be displayed directly by angle-resolved photoemission.[31] The splitting was probed by spin- and angle-resolved photoemission at 1.15 eV binding energy.[30] Along the $\overline{K}$-$\overline{\Gamma}$ direction, the splitting vanishes, whereas perpendicular to this direction it reached 200 meV. Based on this anisotropy, an even stronger splitting was predicted along the $\overline{K}$-$\overline{M}$ direction. Several possible reasons for an externally

enhanced spin-orbit splitting have been discussed, such as buckling and compressive strain in the graphene grown on SiC(0001) as well as defects.[30]

Due to its potential importance we have conducted our own extensive investigation of this effect. In a paper on quasifreestanding graphene/H/SiC, where the influence of the SiC substrate is largely suppressed, the authors indicate that they cannot identify the origin of the measured polarization signal.[32] As the spin-orbit splitting and its anisotropy are still unclear in this system and because we recently observed a Rashba splitting of ∼100 meV for the $p(9 \times 9)$ phase of Au-intercalated graphene/Ni(111) (Ref. 33) and ∼50 meV for the $R0^\circ$ phase of graphene/Ir(111),[34] we want to report on our results in the following.

We have grown monolayer graphene samples on the Si-face of nitrogen-doped ($[N] = 1$–2×10^{18} cm^{-3}) 6H-SiC(0001) as described in Ref. 35. At first, the substrate was etched in molecular hydrogen at a pressure of 1 bar and a temperature of 1550 °C to remove polishing damage. Then a monolayer of graphene was grown by annealing the sample in 1 bar of argon at a temperature of 1650 °C for 15 min. The coverage of one monolayer was confirmed by x-ray photoelectron spectroscopy. Two samples A and B were then transferred in air to the spin- and angle-resolved photoemission setup and cleaned *in situ* by annealing to temperatures below 1000 °C.

Spin- and angle-resolved photoemission has been performed with a hemispherical analyzer coupled to a Rice University Mott-type spin polarimeter operated at 26 kV sensitive to the in-plane spin component.[36] Linearly polarized synchrotron light from the UE112-PGM1 undulator beamline at BESSY II has been used for excitation of photoelectrons. Data shown here are for a photon energy of 55 eV and p polarization. The light-incidence angle was 45°. Overall energy (of electrons and photons) and angular resolution of the experiments was 80 meV and 1°. The base pressure was 2×10^{-10} mbar, and the experiments were done at room temperature. Angle-resolved photoemission revealed the characteristic dispersion of massless Dirac fermions[31] with a Dirac point ∼420 meV below E_F.

Spin- and angle-resolved photoemission can, with the same sort of apparatuses, be performed at constant kinetic energy (constant binding energy) while scanning the electron emission angle, providing momentum-distribution curves as was done in Ref. 30 or taking an energy spectrum at fixed electron emission angle as done in the present work. The maxima are broad due to the limited angle resolution of the detector in conjunction with the large group velocity which is proportional to dE/dk. The determination of the spin-orbit splitting by spin-resolved photoemission is principally possible with very high accuracy due to the fact that the photoemission spectra are counted by separate counters. In particular, the measurable splitting is not limited by the energy resolution but by the acquired statistics and systematic errors. Because of the strong predicted anisotropy of the spin splitting,[30] we sample a substantial number of **k** points in different directions around the $\overline{\mathrm{K}}$ point. Because spin-resolved measurements are time consuming, we limited the acquisition time for each measurement to allow for statistical and systematic errors below 20 meV. We do not observe a measurable spin splitting, which renders the question for the accuracy of our results most important. We will at first discuss the statistical error and then systematic errors and derive from both the upper limit of the spin-orbit splitting in graphene/SiC from our measurement.

Each individual measurement, i.e., each **k** point, gives four spin-resolved spectra, $I_x^\uparrow(E)$, $I_x^\downarrow(E)$, $I_y^\uparrow(E)$, and $I_y^\downarrow(E)$, where E is the binding energy. For each measurement, the spin-orbit splittings of the π band $\Delta_{\mathrm{SO},x}$ and $\Delta_{\mathrm{SO},y}$ for spin quantization along x ($\|\overline{\Gamma\mathrm{K}}$) and y ($\perp\overline{\Gamma\mathrm{K}}$), respectively, have been determined as follows: As the lineshape in angle-resolved photoemission is not defined as straightforwardly as, e.g., in core-level photoemission, we decided not to fit the π-peak shape but to calculate the centroid of the π peak after subtraction of the background, i.e., $E^\uparrow_{\mathrm{cent},x} = \frac{\sum[E\ I_x^\uparrow(E)]}{\sum I_x^\uparrow(E)}$, where the sum is over all data points in the peak. The resulting splittings are then $\Delta_{\mathrm{SO},x} = E^\uparrow_{\mathrm{cent},x} - E^\downarrow_{\mathrm{cent},x}$ and $\Delta_{\mathrm{SO},y} = E^\uparrow_{\mathrm{cent},y} - E^\downarrow_{\mathrm{cent},y}$.

An alternative approach for determining the splitting has been used as well. In this case the splitting $\Delta_{\mathrm{SO},x}$ (same for y) is an average over spin splittings $\Delta_{i,x}$ for every data point on the sides of the peak, $\Delta_i = E_i^\uparrow - E_i^\downarrow$. $E^\uparrow_{i,x}$ and $E^\downarrow_{i,x}$ are determined from the condition $I^\uparrow_{i,x}(E^\uparrow_{i,x}) = I^\downarrow_{i,x}(E^\downarrow_{i,x})$ by linear interpolation in order to assure a one-to-one correspondence between data points in the spin-up and spin-down spectra. Both approaches gave the same results for Δ_{SO} for all **k** points. The statistical error σ_x has then been calculated as the standard deviation of the mean value $\Delta_{\mathrm{SO},x}$.

We found that σ_x and σ_y become so small that they are of the order of the systematic errors of the experiment. The systematic error of the spin-resolved photoemission spectrum results mainly from the sample alignment for an individual measurement, and it changes for each new **k** point since each new **k** point requires a new sample alignment. One possible way to control this systematic error is to reverse the spin splitting by subsequently comparing $+\mathbf{k}$ with $-\mathbf{k}$ as we did for the Rashba-type spin-orbit splitting in Ref. 21. This is not possible in the present experiment because we do not observe a Rashba splitting. In each measurement we sampled a different **k** point, therefore we cannot reduce the systematic error $\delta\Delta_{\mathrm{SO}}$ below the measured value for the spin splitting, i.e., $\delta\Delta_{\mathrm{SO}} = |\Delta_{\mathrm{SO}}|$. Therefore, the upper limit of the spin splitting at each **k** point is $\delta_{\mathrm{UL},x} = |\Delta_{\mathrm{SO},x}| + \sigma_x$.

We took particular care to sample both supposed[30] areas of large and small splitting. Our nine probed **k** points are marked in Fig. 1 by green (+, sample A) and yellow crosses (×, sample B). The upper limits of the spin splittings are shown there separately for the two spin quantization directions in the graphene plane x [$\|\overline{\Gamma\mathrm{K}}$, Fig. 1(a)] and y [$\perp\overline{\Gamma\mathrm{K}}$, Fig. 1(b)] which the present experiment probes. The upper limits are ∼20 meV or less.

Figures 2(a) and 2(b) show data from sample A at $\mathbf{k}_1$. Parts (a) and (b) display data for the above mentioned two perpendicular spin quantization axes. No splitting of the π peak appears in either of the two. Parts (c) and (d) show data from sample B at $\mathbf{k}_2$, where the maximum splitting was predicted but which has not been probed before.[30] Parts (e) and (f) show a measurement from sample B at $\mathbf{k}_3$ where 200 meV splitting was reported at first. Only the π peak is measured here but with improved statistics. No splitting is seen. Other data points shown in Fig. 1

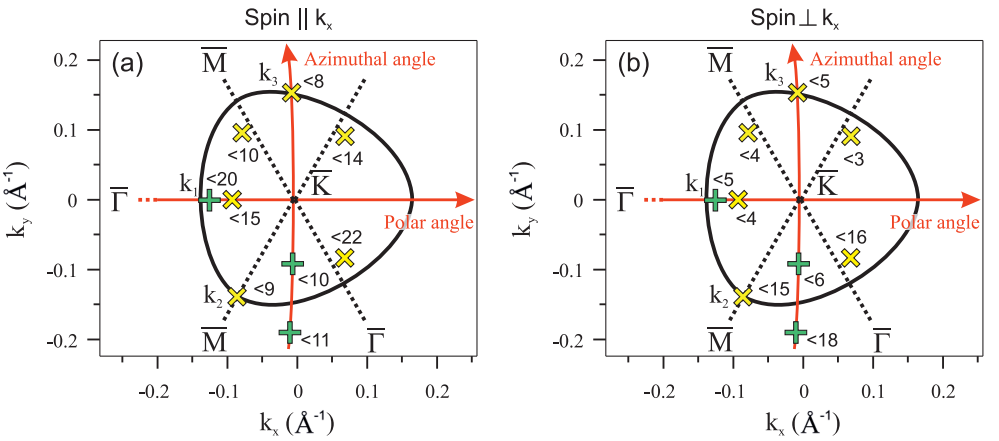

FIG. 1. (Color online) Region near the $\overline{\mathrm{K}}$ point of the graphene Brillouin zone with calculated constant energy surface (at ∼0.8 eV below the Dirac point) and measurements of the spin-orbit splitting from sample A (green, +) and sample B (yellow, ×). The upper limit of the spin splitting of each measurement (δ_{UL}, in meV) is given at each measured **k** point separately for spin quantization axes (a) along x (parallel to $\overline{\Gamma\mathrm{K}}$) and (b) along y (perpendicular to $\overline{\Gamma\mathrm{K}}$). Labels k_1, k_2, and k_3 denote the data points corresponding to Fig. 2.

have been measured from the two samples with the same result. The spectra have been analyzed by the procedure explained in the text above and no splitting is observed with the confidence limit being of the order of 20 meV.

To estimate the size of Rashba-type spin-orbit splitting for graphene on SiC we performed density functional theory calculations in the generalized gradient approximation[37] using the full-potential linearized augmented plane-wave method.[38] For simplicity, we assumed a geometry matching a $p(2 \times 2)$ graphene unit cell to a $(\sqrt{3} \times \sqrt{3})R30^\circ$ unit cell of 6H-SiC(0001), similarly to the model employed in Ref. 39 with two carbon layers on the SiC. The substrate was modeled by a film of six bilayers of SiC where the dangling bonds of the lower surface were saturated with H. The structural parameters were taken from Ref. 39. Although the structural model can be refined,[40] it is reasonable to assume that the present model captures the spin-orbit effects in this system quite well.

We compared three different SiC terminations: Si- and C-terminated ones, as well as a C-terminated substrate with a C-deficient interface layer. We observe band structures similar

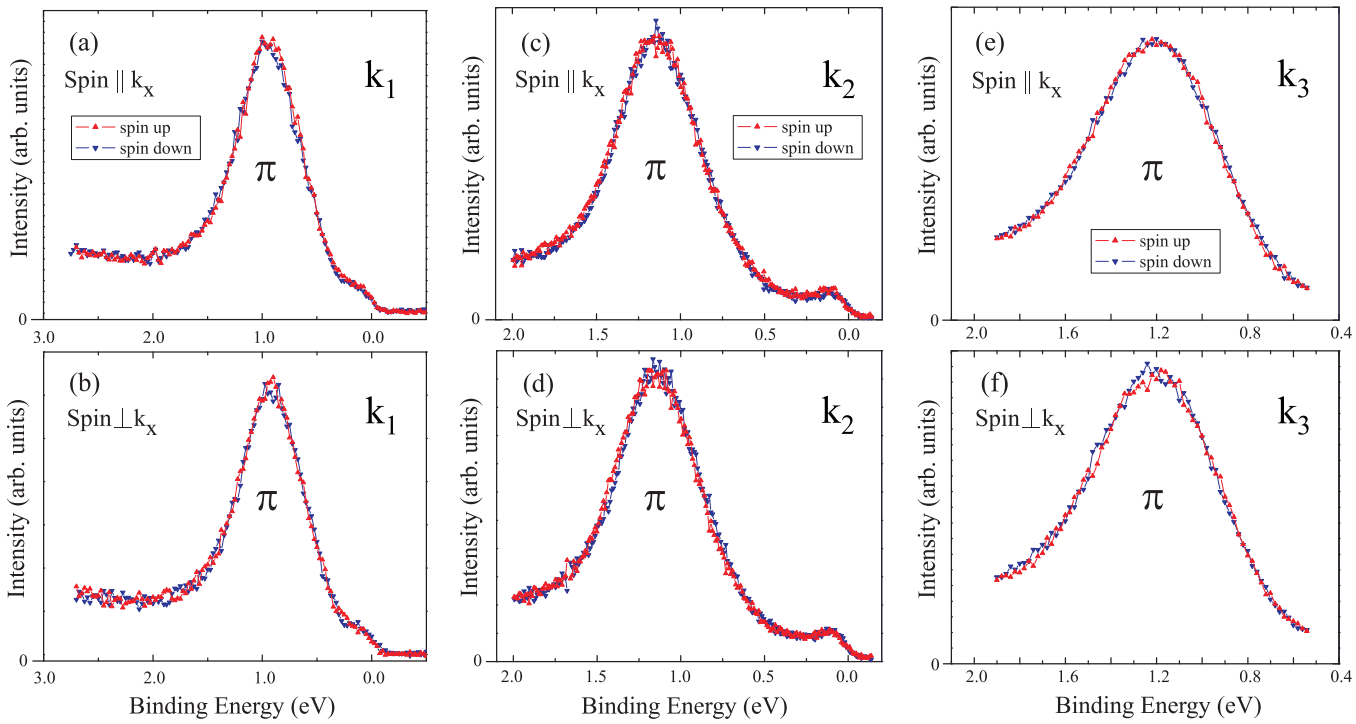

FIG. 2. (Color online) (a),(b) Spin- and angle-resolved photoemission for sample A with **k** along the $\overline{\Gamma\mathrm{K}}$ line where no splitting was predicted. Parts (a) and (b) refer to the two orthogonal spin quantization axes in the graphene plane. (c),(d) Same as (a),(b) but for sample B and **k** along $\overline{\mathrm{KM}}$ where maximum spin-orbit splitting has been predicted. (e),(f) Same as (c),(d) but for **k** along the direction perpendicular to $\overline{\Gamma\mathrm{K}}$ where 200 meV spin-orbit splitting has been reported. The spin splitting in the present figure is less than 10 meV.

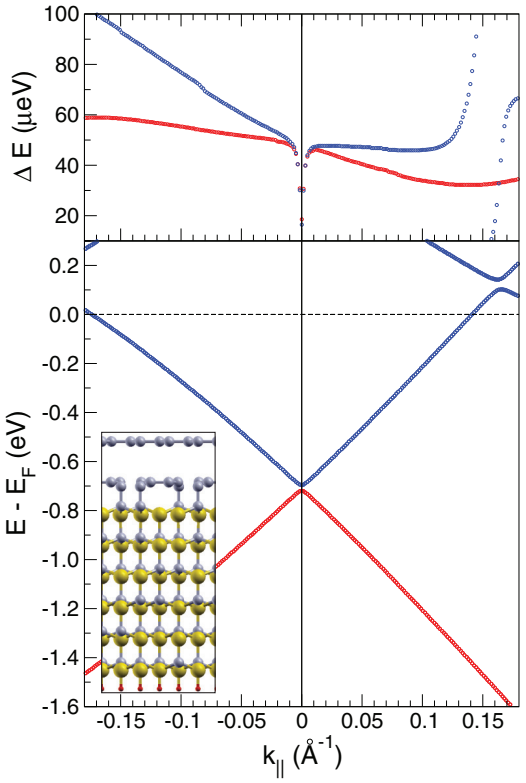

FIG. 3. (Color online) Lower panel: p_z band of graphene on a C-terminated SiC substrate with a C-deficient interface layer. The inset shows the structural model (the lower surface of the film is passivated with hydrogen) with Si, C, and H atoms indicated by large, medium, and small spheres. $k_\parallel = 0$ indicates the $\overline{\mathrm{K}}$ point, negative $k_\parallel$ values signify the direction towards $\overline{\Gamma}$, positive $k_\parallel$ values towards $\overline{\mathrm{M}}$. Upper panel: Spin-orbit splitting of the upper (blue) and lower branch (red) of the Dirac cone formed by the p_z band. At the $\overline{\mathrm{K}}$ point, the splitting reduces to about 20 μeV; at a band crossing at around 0.15 Å^{-1} it can reach more than 0.1 meV.

to the calculations in Ref. 39: for the C- and Si-terminated surfaces the Dirac cone is near and below the Fermi level, respectively. In both cases an almost dispersionless state is pinned at the Fermi level, while in the calculations with the C-deficient interface layer this state is dispersive and mainly located above the Fermi level (in Fig. 3 visible at about $+0.2$ eV). In all three cases the Rashba-type spin-orbit splitting of the valence-band part of the p_z bands at the $\overline{\mathrm{K}}$ point was far below the experimental resolution limits. Slight variations of this value come from the different surface terminations, ranging from 0.02 meV for the Si- and C-terminated surface to 0.05 meV for the C-deficient one. According to the model of spin-orbit splitting in graphene[13,24] this value is the Bychkov-Rashba contribution, i.e., the part that is induced by the substrate. In addition, there is an intrinsic spin-orbit splitting for graphene that is in the same order of magnitude: our calculations predict a value of 25 μeV, in good agreement with previous calculations.[13] As mentioned above, we see a dangling bond near the Fermi level which is for the C-deficient surface mainly unoccupied. Where this band crosses the Dirac cone, we see a deformation of the state (i.e., a deviation from sp^2 hybridization) and it extends towards the C-deficient layer. Any deviation from the pure p_z character helps to increase the spin-orbit splitting in the π band; here we observe locally an enhancement of the spin-orbit splitting by a factor of 5–10. Finally, we investigated the anisotropy of the splitting, i.e., the fact that the spin-orbit splitting of the occupied branches is not constant and even develops differently along $\overline{\mathrm{K}\Gamma}$ and $\overline{\mathrm{KM}}$. Due to the fact that the intrinsic spin-orbit splitting is of the same order as the Bychkov-Rashba splitting, a significant **k** dependence can be expected around the $\overline{\mathrm{K}}$ point and sharp variations were indeed observed.

Also with a larger energy and momentum range, the spin-orbit splitting is found to vary up to 50%: As an example, we show in Fig. 3 the Dirac cone formed by the p_z band of graphene on a C-terminated SiC substrate with a C-deficient interface layer. Indeed, the branches show a different evolution of the spin-orbit splitting in directions $\overline{\mathrm{K}\Gamma}$ (negative $k_\parallel$ values) and $\overline{\mathrm{KM}}$ (positive $k_\parallel$ values) that is, moreover, dependent on the branch of the p_z band. The upward dispersing branch shows a rather constant splitting of 50–60 μeV until it crosses another band at 0.15 Å^{-1}, where the splitting gets significantly enhanced. The downward dispersing branch starts at -0.17 Å^{-1} with a comparatively large spin-orbit splitting of 100 μeV that drops to 35 μeV in the direction $\overline{\mathrm{KM}}$. We have to note, however, that the absolute value of these effects is small and depends strongly on the surface termination and details of the relaxation. The errors introduced with our simplified structural model are probably affecting the results on this level.

We had earlier shown that there is no sizable Rashba effect in graphene/Ni(111) and no exchange splitting around the center of the graphene π band[41] and that this does not change for graphene/Co(0001).[42] We find the present results in agreement with our previous conclusion that a sizable Rashba splitting in graphene requires proximity to a heavy element such as Au.[21] Actually, it has recently been demonstrated that the system graphene/SiC(0001) can be intercalated with a Au monolayer.[43,44] This would be a promising semiconductor system for achieving a Rashba-type spin-orbit splitting at the Fermi level in graphene.

This work was supported by SPP 1459 of the Deutsche Forschungsgemeinschaft. A.R. acknowledges support by DAAD within the G-RISC program.

*Present address: Physikalische und Theoretische Chemie, Institut für Chemie und Biochemie, Freie Universität Berlin, Takustraße 3, 14195 Berlin, Germany.

[1] A. H. Castro Neto, F. Guinea, N. M. R. Peres, K. S. Novoselov, and A. K. Geim, Rev. Mod. Phys. **81**, 109 (2009).

[2] K. I. Bolotin, K. J. Sikes, J. Hone, H. L. Stormer, and P. Kim, Phys. Rev. Lett. **101**, 096802 (2008).

[3] O. V. Yazyev, Rep. Prog. Phys. **73**, 056501 (2010).

[4] J. M. D. Coey, M. Venkatesan, C. B. Fitzgerald, A. P. Douvallis, and I. S. Sanders, Nature (London) **240**, 156 (2002).

[5]P. Esquinazi, A. Setzer, R. Höhne, and C. Semmelhack, Y. Kopelevich, D. Spemann, T. Butz, B. Kohlstrunk, and M. Lösche, Phys. Rev. B **66**, 024429 (2002).
[6]P. Esquinazi, in *Handbook of Magnetism and Advanced Magnetic Materials*, edited by H. Kronmüller and S. Parkin (Wiley, Chichester, 2007).
[7]H. Ohldag, T. Tyliszczak, R. Höhne, D. Spemann, P. Esquinazi, M. Ungureanu, and T. Butz, Phys. Rev. Lett. **98**, 187204 (2007).
[8]H.-Ch. Mertins, S. Valencia, W. Gudat, P. M. Oppeneer, O. Zaharko, and H. Grimmer, Europhys. Lett. **66**, 743 (2004).
[9]M. Weser, Y. Rehder, K. Horn, M. Sicot, M. Fonin, A. B. Preobrajenski, E. N. Voloshina, E. Goering, and Y. S. Dedkov, Appl. Phys. Lett. **96**, 012504 (2010).
[10]A. Varykhalov, D. Marchenko, J. Sánchez-Barriga, M. R. Scholz, B. Verberck, B. Trauzettel, T. O. Wehling, C. Carbone, and O. Rader, Phys. Rev. X **2**, 041017 (2012).
[11]C. L. Kane and E. J. Mele, Phys. Rev. Lett. **95**, 226801 (2005).
[12]J. C. Boettger and S. B. Trickey, Phys. Rev. B **75**, 121402 (2007).
[13]M. Gmitra, S. Konschuh, C. Ertler, C. Ambrosch-Draxl, and J. Fabian, Phys. Rev. B **80**, 235431 (2009); S. Abdelouahed, A. Ernst, J. Henk, I. V. Maznichenko, and I. Mertig, *ibid*. **82**, 125424 (2010).
[14]R. Winkler and U. Zülicke, Phys. Rev. B **82**, 245313 (2010).
[15]J. C. Slonczewski and P. R. Weiss, Phys. Rev. **109**, 272 (1958).
[16]N. Tombros, C. Jozsa, M. Popinciuc, H. T. Jonkman, and B. van Wees, Nature (London) **448**, 571 (2007).
[17]S. Cho, Y.-F. Chen, and M. S. Fuhrer, Appl. Phys. Lett. **91**, 123105 (2007).
[18]Wei Han, W. H. Wang, K. Pi, K. M. McCreary, W. Bao, Yan Li, F. Miao, C. N. Lau, and R. K. Kawakami, Phys. Rev. Lett. **102**, 137205 (2009).
[19]D. Huertas-Hernando, F. Guinea, and A. Brataas, Phys. Rev. B **74**, 155426 (2006).
[20]F. Kuemmeth, S. Ilani, D. C. Ralph, and P. L. McEuen, Nature (London) **452**, 448 (2008).
[21]A. Varykhalov, J. Sánchez-Barriga, A. M. Shikin, C. Biswas, E. Vescovo, A. Rybkin, D. Marchenko, and O. Rader, Phys. Rev. Lett. **101**, 157601 (2008).
[22]S. Murakami, A. Nagaosa, and S.-C. Zhang, Science **301**, 1348 (2003).
[23]J. Sinova, D. Culcer, Q. Niu, N. A. Sinitsyn, T. Jungwirth, and A. H. MacDonald, Phys. Rev. Lett. **92**, 126603 (2004).
[24]E. I. Rashba, Phys. Rev. B **79**, 161409(R) (2009).
[25]F. Kuemmeth and E. I. Rashba, Phys. Rev. B **80**, 241409 (2009).
[26]H. Min, J. E. Hill, N. A. Sinitsyn, B. R. Sahu, L. Kleinman, and A. H. MacDonald, Phys. Rev. B **74**, 165310 (2006).
[27]M. Zarea and N. Sandler, Phys. Rev. B **79**, 165442 (2009).
[28]C. R. Ast and I. Gierz, Phys. Rev. B **86**, 085105 (2012).
[29]A. Varykhalov, M. R. Scholz, Timur K. Kim, and O. Rader, Phys. Rev. B **82**, 121101(R) (2010).
[30]I. Gierz, J. H. Dil, F. Meier, B. Slomski, J. Osterwalder, J. Henk, R. Winkler, C. R. Ast, and K. Kern, arXiv:1004.1573v1 (2010).
[31]A. Bostwick, T. Ohta, T. Seyller, K. Horn, and E. Rotenberg, Nat. Phys. **3**, 36 (2007).
[32]I. Gierz, J. H. Dil, F. Meier, B. Slomski, J. Osterwalder, J. Henk, R. Winkler, C. R. Ast, and K. Kern, arXiv:1004.1573v2 (2011).
[33]D. Marchenko, A. Varykhalov, M. R. Scholz, G. Bihlmayer, E. I. Rashba, A. Rybkin, A. M. Shikin, and O. Rader, Nat. Commun. **3**, 1232 (2012).
[34]D. Marchenko, J. Sánchez-Barriga, M. R. Scholz, O. Rader, and A. Varykhalov, Phys. Rev. B **87**, 115426 (2013).
[35]K. V. Emtsev, A. Bostwick, K. Horn, J. Jobst, G. L. Kellogg, L. Ley, J. McChesney, T. Ohta, S. A. Reshanov, J. Röhrl, E. Rotenberg, A. K. Schmid, D. Waldmann, H. B. Weber, and Th. Seyller, Nat. Mater. **8**, 203 (2009).
[36]G. C. Burnett, T. J. Monroe, and F. B. Dunning, Rev. Sci. Instrum. **65**, 1893 (1994).
[37]J. P. Perdew and K. Burke and M. Ernzerhof, Phys. Rev. Lett. **77**, 3865 (1996).
[38]For a program description see http://www.flapw.de.
[39]F. Varchon, R. Feng, J. Hass, X. Li, B. N. Nguyen, C. Naud, P. Mallet, J.-Y. Veuillen, C. Berger, E. H. Conrad, and L. Magaud, Phys. Rev. Lett. **99**, 126805 (2007).
[40]S. Kim, J. Ihm, H. J. Choi, and Y.-W. Son, Phys. Rev. Lett. **100**, 176802 (2008).
[41]O. Rader, A. Varykhalov, J. Sánchez-Barriga, D. Marchenko, A. Rybkin, and A. M. Shikin, Phys. Rev. Lett. **102**, 057602 (2009).
[42]A. Varykhalov and O. Rader, Phys. Rev. B **80**, 035437 (2009).
[43]B. Premlal, M. Cranney, F. Vonau, D. Aubel, D. Casterman, M. M. De Souza, and L. Simon, Appl. Phys. Lett. **94**, 263115 (2009).
[44]I. Gierz, T. Suzuki, R. Th. Weitz, D. S. Lee, B. Krauss, C. Riedl, U. Starke, H. Höchst, J. H. Smet, C. R. Ast, and K. Kern, Phys. Rev. B **81**, 235408 (2010).